

Dark energy constraints from quasar observations

B. Czerny^{1*}, M.L. Martínez-Aldama¹, G. Wojtkowska², M. Zajaček¹, P. Marziani³, D. Dultzin⁴, M. H. Naddaf¹, S. Panda¹, R. Prince¹, R. Przyluski⁵, M. Ralowski⁶, and M. Śniegowska¹

¹Center for Theoretical Physics, Polish Academy of Sciences, Al. Lotników 32/46, 02-668 Warsaw, Poland

²Warsaw University Observatory, Al. Ujazdowskie 4, 00-478 Warszawa, Poland

³INAF, Osservatorio Astronomico di Padova, Italy

⁴Instituto de Astronomía, UNAM, Mexico

⁵Space Research Centre, Polish Academy of Sciences, Bartycka 18a, 00-716 Warsaw, Poland

⁶Astronomical Observatory of the Jagiellonian University, Orla 171, 30-001 Krakow, Poland

*Corresponding author: B. Czerny, bcz@cft.edu.pl

Key words: cosmology, dark energy, quasars

Abstract

Recent measurements of the parameters of the Concordance Cosmology Model (Λ CDM) done in the low-redshift Universe with Supernovae Ia/Cepheids, and in the distant Universe done with Cosmic Microwave Background (CMB) imply different values for the Hubble constant (67.4 ± 0.5 [km s⁻¹ Mpc⁻¹] from Planck vs 74.03 ± 1.42 [km s⁻¹ Mpc⁻¹] Riess et al. 2019). This Hubble constant tension implies that either the systematic errors are underestimated, or the Λ CDM does not represent well the observed expansion of the Universe. Since quasars - active galactic nuclei - can be observed in the nearby Universe up to redshift $z \sim 7.5$, they are suitable to estimate the cosmological properties in a large redshift range. Our group develops two methods based on the observations of quasars in the late Universe up to redshift $z \sim 4.5$, with the objective to determine the expansion rate of the Universe. These methods do not yet provide an independent measurement of the Hubble constant since they do not have firm absolute calibration but they allow to test the Λ CDM model, and so far no departures from this model were found.

1 Introduction

The cosmological parameters can be estimated from different sets of data at various redshifts, but if the standard Λ CDM (Lambda-Cold Dark Matter) model is valid, they can always be represented by the current (zero redshift) values. The final results from the Planck mission, based on the analysis of the Cosmic Microwave Background (CMB) do not indicate any tension with the standard model, and give the value of the $\Omega_m = 0.315 \pm 0.007$ [1] and the Hubble constant $H_0 = 67.4 \pm 0.5$ [km s⁻¹ Mpc⁻¹]. Many of the measurements done in the local Universe ($z < 10$) are in significant disagreement with

these Ω_m or H_0 values (e.g. [2]) while other measurements, also local, are still roughly in agreement with the results from Planck (e.g. the last results from gravitational waves [3]).

Therefore various probes and methods are needed to confirm, or to reject, the hypothesis that the Λ CDM model does not well describe the Universe, and the evolving dark energy is needed instead of the cosmological constant. Quasars (QSO) are very attractive cosmological probes, since they cover a broad range of redshifts, from nearby sources (referred to as Active Galactic Nuclei, AGN) to most distant objects at redshift above 7 [4, 5]. They also

do not show significant evolution with redshift [6].

2 Two methods for using quasars in cosmology

We are currently using two methods of turning quasars into *standardizable* candles. The first method is based on the radius-luminosity relation and the second method is based on super-Eddington sources.

2.1 Method based on radius-luminosity relation for the BLR

The reverberation mapping technique is based on the long-term monitoring of a source in order to determine the time response (τ_{BLR}) of the emission line to the continuum variations [7]. The most important result from the reverberation mapping studies is the correlation between the continuum luminosity (L) and the distance (R_{BLR}) where the emission line is emitted in the broad line region (BLR). This relation is known as the Radius-Luminosity relation (RL) and it is given approximately by $R_{\text{BLR}} \propto L^{0.5}$. The reverberation mapping studies require extensive use of telescope time to achieve high quality results, thus only ~ 120 sources have been analyzed with this technique until date. Most of the monitoring are based on the optical $\text{H}\beta$ for low-redshift sources, while for high redshift regimes, due to the Doppler shift, the monitoring are focused on the UV emission lines such as $\text{Mg II } \lambda 2800$, $\text{C IV } \lambda 1549$ and $\text{C III } \lambda 1909$.

For many years the RL relation showed a low scatter ($\sigma_{\text{rms}} \sim 0.13$ dex) [8], which ensured its use in the determination of the black hole mass (M_{BH}). However, the inclusion of new sources, particularly those radiating close to the Eddington limit (high accretion rates), has led to a much larger scatter, clearly related with the accretion rate [9, 10]. Some corrections based on the accretion rate [11] and independent parameters such as the Fe II strength or the amplitude of variability [12, 13, 14] (in turn correlated with the accretion rate) have been proposed to correct this effect, allowing to reduce the scatter.

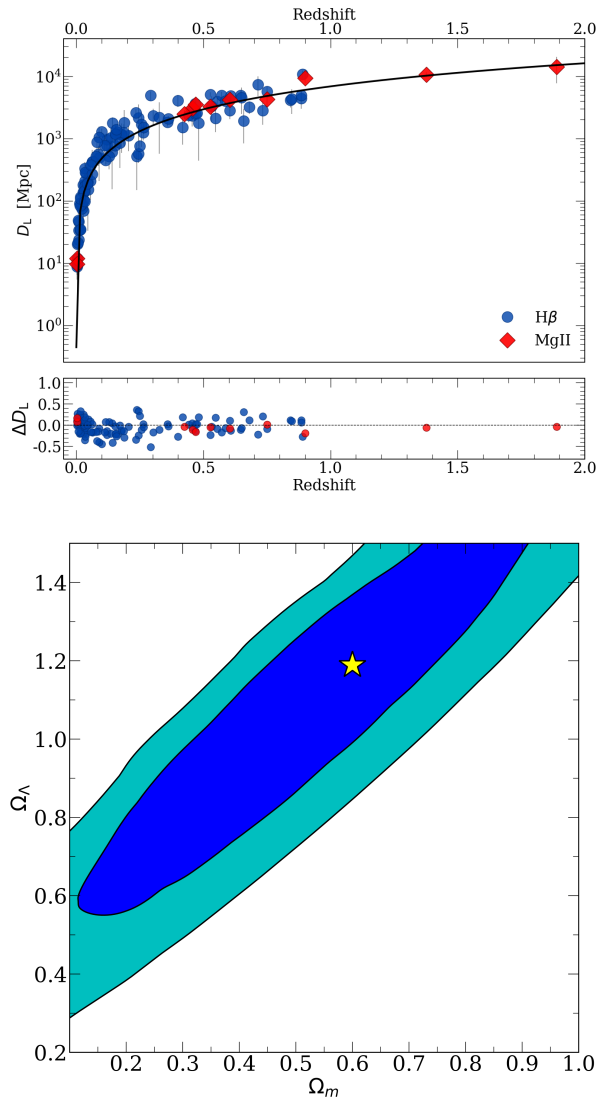


Figure 1: Top panel: Quasar Hubble diagram using the reverberation mapped sources. Blue circles and red diamonds correspond to the $\text{H}\beta$ and $\text{Mg II } \lambda 2800$ sources, respectively. Black line marks the ΛCDM model for flat cosmology, $\Omega_m = 0.297$, $H_0 = 67.5$ $[\text{km s}^{-1} \text{Mpc}^{-1}]$. Bottom subpanel shows the residuals. Bottom panel: Confidence contours at 68% (cyan) and 95% (blue) for Ω_m and Ω_Λ for general ΛCDM model based on χ^2 fitting where the best Ω_m and Ω_Λ are represented by the yellow symbol.

Besides, the Radius-Luminosity relation offers the possibility to determine the luminosity independently of the redshift [15, 16], and to estimate the cosmological parameters. However, in [11] the errors for Ω_m and Ω_Λ based on available $\text{H}\beta$ were still very large, despite the corrections for the accretion

rate. In the present paper, we make the following important modifications. First, we combine the previous sample with Mg II $\lambda 2800$ reverberation-mapped sources. The new sample includes two sources monitored by us with The Southern African Large Telescope (SALT) during 6 years [17, 18]. Next, since the errors of the time delay measurement are highly asymmetric, we use the χ^2 statistics to determine the cosmological parameters, we use the method of [19] instead of a simple symmetrization of the errors.

We also modified the approach to the R-L relation in case of the $H\beta$ sample which is extremely heterogeneous. We treated the coefficients of this relation as arbitrary, and minimized the total χ^2 fit to a flat cosmological model, with Hubble constant fixed at $67.5 \text{ [km s}^{-1} \text{ Mpc}^{-1}]$. For Mg II $\lambda 2800$ sample, we used the R-L parametrization given by Eq. 9 in [18] since this sample was analysed in a more uniform way. While fitting the flat cosmology model (both samples combined), we applied the sigma-clipping approach, and we removed the sources which showed a departure by more than 3 sigma from the best-fit. All the removed sources were from the $H\beta$ sample: Mrk 493, J074352.02+271239.5, Mkn 509, MCG+08-11-011, J142103, J142043, J141123, and J142052. Thus our total sample has now 120 objects. We then refitted the Hubble diagram. The best-fit returned the best R-L parametrization of $H\beta$ sample as $\log L_{5100} = 1.489 \log \tau_{\text{corr}} - 2.222$, where τ_{corr} is the time delay corrected by the accretion rate effect [11]. For the flat cosmology, we obtained the best-fit value $\Omega_m = 0.297^{+0.060}_{-0.054}$ (see Fig. 1, top panel). This value is fully consistent with the value 0.3153 ± 0.0073 from Planck [1] for flat cosmology, and the error in our new result is much smaller than obtained by [11], although still much larger than from Planck. This illustrates that the method could be powerful, if the sample is more uniformly analysed from the very beginning. If we do not assume a flat cosmology, 2-D contour errors are still large (see Fig. 1, bottom panel), although considerably smaller than in [11]. The best-fit Planck values are well within the 1σ error, so we do not see any tension with the results based on Cosmic Microwave Background.

2.2 Method based on Super-Eddington sources

Quasars radiating close to the Eddington limit are known as xA-QSO or super-Eddington sources [20, 21]. This QSO population shows peculiar spectral and photometric properties, which differenti-

ate them from the rest of the QSO population and make them easy to identify in catalogs like SDSS or the upcoming Vera Rubin Observatory’s Legacy Survey of Space and Time (LSST). In the optical range, they are the strongest Fe II emitters and do not show a strong contribution of narrow emission lines such as [O III] $\lambda\lambda 4959, 5007$ [22]. xA-QSO show the strongest outflows in the high ionization lines mostly observed in the UV emission lines like C IV $\lambda 1549$ or S IV $\lambda 1397$ [23], although in the most extreme cases the strong radiation forces provoke the presence of outflows in low-ionization lines such as $H\beta$ or Al III $\lambda 1860$. According to the photoionization models, their broad line regions show large densities ($n_H = 10^{12-13} \text{ [cm}^{-3}]$), low-ionization parameters ($\log U < -2$) and high metallicities ($Z \sim 10Z_\odot$) [24, 25, 26, 27]. In addition, Super-Eddington sources also show remarkably low optical variability and time delays shorter than the predicted by the RL relation [28]. The UV flux ratios Al III $\lambda 1860$ /Si III $\lambda 1892 > 0.5$ and C III $\lambda 1909$ /Si III $\lambda 1892 < 1.0$ have shown a high effectiveness as selection criteria to identify xA-QSO sources at high-redshift, while at-low redshift xA-QSO typically show Fe II/ $H\beta > 1.0$ [20].

In xA-QSO, despite the rise of the accretion rate, the luminosity saturates toward a limiting value, since the accretion efficiency decreases. Thus the ratio luminosity–black hole mass (L/M_{BH}) does not change and they can be considered as “Eddington standard candles”. A similarity in the physical conditions (density, ionization parameter, metallicity) of the BLR is expected because them belonging to the same population, therefore a generalization of all of them can be considered [29]. Since the low-ionization lines are less affected by the strong radiation forces, emission lines like $H\beta$ and Al III $\lambda 1860$ are excellent candidates for virial estimators. Based on these assumptions, it is possible to determine the luminosity distances independently of redshift and get an estimation of the matter and energy content in the Universe.

The previous xA-QSO sample included ~ 200 objects at redshift $z < 2.7$ [30]. In order to increase the redshift range, we considered the most recent edition of the The Sloan Digital Sky Survey Reverberation Mapping (SDSS-RM) catalog [31]. This catalog includes the automatic measurements of the most important UV emission lines for 549 sources with $44.1 < \log L_{1700} < 46.9 \text{ [erg s}^{-1}]$ at $0.9 < z < 4.3$, where $\sim 20\%$ show high accretion rates, so they can be considered as Super-Eddington candidates. In the xA sources the Fe III $\lambda 1914$ shows

an important contribution, hence a good deblending of the C III] $\lambda 1909$ and Fe III $\lambda 1914$ is required. Unfortunately, the SDSS catalog does not include Fe III in their multicomponent fittings, so not all the sources satisfy the selection criteria to identify them as the xA. So for the first test, we select the sources based on the Eddington ratio ($L/L_{\text{Edd}} > 0.2$) estimated from the Al III $\lambda 1860$ based black hole mass. After removal of some objects with extreme $\text{FWHM}_{\text{AlIII}}$ values, our final sample includes 88 objects at $1 < z < 4.5$.

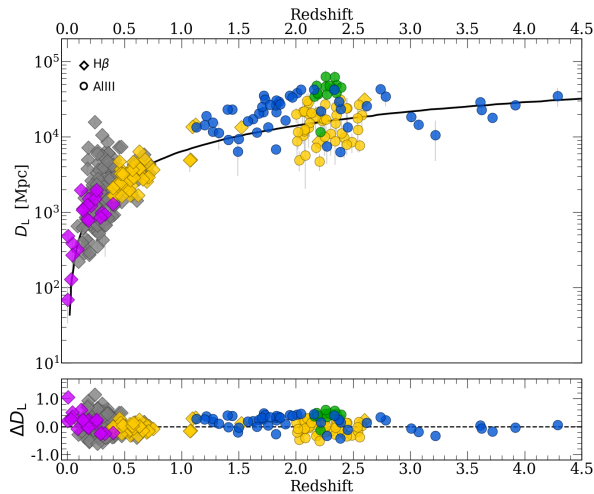


Figure 2: Quasar Hubble diagram using the Super-Eddington sources. Diamonds correspond to the measurements from the $H\beta$, while circles belong to UV Al III $\lambda 1860$ emission line. Purple, gray, yellow, green and blue symbols correspond to the xA sources from the SEAMBH project [12], [22], [20], [25] and SDSS-RM [31] samples, respectively. The best-fit line shows the flat model, with H_0 from Planck, and best fit $\Omega_m = 0.290$.

In order to determine the cosmological constant Ω_m and Ω_Λ , we combine the previous xA samples such as the super-Eddington sources from the super-Eddington accreting massive black holes (SEAMBHs) project with the most recent measurements from [25]. The quasar Hubble diagram with the super-Eddington sources is shown in Fig. 2. We adopt the scaling of the virial estimator to be consistent with Planck H_0 value, and we assume the flat cosmology. In this case we obtain $\Omega_m = 0.290^{+0.048}_{-0.043}$, fully consistent with the Planck results despite the fact that quasars cover the redshift range from nearby sources to almost 4.5.

3 Discussion

Here we presented the most recent results based on the two methods for applying quasars to constrain the expansion rate of the Universe. Our methods, as for now, are not based on absolute scaling so they cannot predict the value of H_0 . In principle, such an absolute scaling can be achieved. For method (i) it would require an independent measurement of the dust temperature at the BLR onset, and the development of a 3-D BLR model, which is in progress (see e.g. [32]). For method (ii), we would need an absolute scaling of the radius-luminosity relation, also establishing the mean density of the BLR (see e.g. [20, 29]). At this stage, we fixed the value of the Hubble constant at the Planck value and tested, whether the redshift dependence of the luminosity distance is consistent with the standard Λ CDM model, and whether the remaining cosmological parameters derived from quasar data are consistent with Planck values.

So far, within the available accuracy, our values of Ω_m are fully consistent with the Planck value for the flat Universe despite the fact that second method extends up to the redshift 4.5. Thus we do not support the claim of the tension with the standard model based on Supernovae Ia with absolute scaling in turn predominantly based on Cepheid stars [33]. Our results from method (i) are consistent with the tension found by [34] since they claim to see departures only above the redshift 1.5 - 2, and method (i) does not go this far. As for the method (ii), we have many sources up to redshift 2.5, but indeed very few above 2.5, and our method of analysis was not yet optimized by an outlier removal through sigma-clipping. Further studies are clearly needed for this method, both with the current data and eventually by increasing the number of high redshift quasars.

Acknowledgement

The project is partially based on observations made with the SALT under programs 2012-2-POL-003, 2013-1-POL-RSA-002, 2013-2-POL-RSA-001, 2014-1-POL-RSA-001, 2014-2-SCI-004, 2015-1-SCI-006, 2015-2-SCI-017, 2016-1-SCI-011, 2016-2-SCI-024, 2017-1-SCI-009, 2017-2-SCI-033, 2018-1-MLT-004 (PI: B. Czerny). The authors acknowledge the financial support by the National Science Centre, Poland, grant No. 2017/26/A/ST9/00756 (Maestro 9), and by the Ministry of Science and Higher Education (MNiSW) grant DIR/WK/2018/12. The Polish

participation in SALT is funded by grant No. MNI SW DIR/WK/2016/07.

References

- [1] Planck Collaboration, N. Aghanim, Y. Akrami, M. Ashdown, J. Aumont, C. Baccigalupi, and et al. Planck 2018 results. VI. Cosmological parameters. *A&A*, 641:A6, September 2020, doi:10.1051/0004-6361/201833910.
- [2] Adam G. Riess. The expansion of the Universe is faster than expected. *Nature Reviews Physics*, 2(1):10–12, December 2019, doi:10.1038/s42254-019-0137-0.
- [3] The LIGO Scientific Collaboration, the Virgo Collaboration, B. P. Abbott, R. Abbott, T. D. Abbott, S. Abraham, F. Acernese, and et al. A gravitational-wave measurement of the Hubble constant following the second observing run of Advanced LIGO and Virgo. *arXiv e-prints*, page arXiv:1908.06060, August 2019.
- [4] D. J. Mortlock, S. J. Warren, B. P. Venemans, M. Patel, P. C. Hewett, . G. McMahon, C. Simpson, and et al. A luminous quasar at a redshift of $z = 7.085$. *Nature*, 474(7353):616–619, June 2011, doi:10.1038/nature10159.
- [5] E. Bañados, B. P. Venemans, C. Mazzucchelli, E. P. Farina, F. Walter, F. Wang, R. Decarli, and et al. An 800-million-solar-mass black hole in a significantly neutral Universe at a redshift of 7.5. *Nature*, 553(7689):473–476, January 2018, doi:10.1038/nature25180.
- [6] M. Onoue, E. Bañados, C. Mazzucchelli, B. P. Venemans, J.-T. Schindler, F. Walter, J. F. Hennawi, and et al. No Redshift Evolution in the Broad-line-region Metallicity up to $z = 7.54$: Deep Near-infrared Spectroscopy of ULAS J1342+0928. *ApJ*, 898(2):105, August 2020, doi:10.3847/1538-4357/aba193.
- [7] B. M. Peterson, L. Ferrarese, K. M. Gilbert, S. Kaspi, M. A. Malkan, D. Maoz, D. Merritt, and et al. Central Masses and Broad-Line Region Sizes of Active Galactic Nuclei. II. A Homogeneous Analysis of a Large Reverberation-Mapping Database. *ApJ*, 613:682–699, October 2004.
- [8] E. Kilerci Eser, M. Vestergaard, B. M. Peterson, K. D. Denney, and M. C. Bentz. On the Scatter in the Radius-Luminosity Relationship for Active Galactic Nuclei. *ApJ*, 801:8, March 2015, doi:10.1088/0004-637X/801/1/8.
- [9] P. Du, C. Hu, K.-X. Lu, Y.-K. Huang, C. Cheng, J. Qiu, and SEAMBH Collaboration. Supermassive Black Holes with High Accretion Rates in Active Galactic Nuclei. IV. $H\beta$ Time Lags and Implications for Super-Eddington Accretion. *ApJ*, 806:22, June 2015, doi:10.1088/0004-637X/806/1/22.
- [10] P. Du, Z.-X. Zhang, K. Wang, Y.-K. Huang, Y. Zhang, K.-X. Lu, and SEAMBH Collaboration. Supermassive Black Holes with High Accretion Rates in Active Galactic Nuclei. IX. 10 New Observations of Reverberation Mapping and Shortened $H\beta$ Lags. *ApJ*, 856:6, March 2018, doi:10.3847/1538-4357/aaae6b.
- [11] M. L. Martínez-Aldama, B. Czerny, D. Kawka, V. Karas, S. Panda, M. Zajaček, and P. T. Życki. Can Reverberation-measured Quasars Be Used for Cosmology? *ApJ*, 883(2):170, October 2019, doi:10.3847/1538-4357/ab3728.
- [12] P. Du and J.-M. Wang. The Radius-Luminosity Relationship Depends on Optical Spectra in Active Galactic Nuclei. *ApJ*, 886(1):42, November 2019, doi:10.3847/1538-4357/ab4908.
- [13] E. Dalla Bontà, B. M. Peterson, M. C. Bentz, W. N. Brandt, S. Ciroi, G. De Rosa, and et al. The Sloan Digital Sky Survey Reverberation Mapping Project: Estimating Masses of Black Holes in Quasars with Single-Epoch Spectroscopy. *arXiv e-prints*, page arXiv:2007.02963, July 2020.
- [14] M. L. Martínez-Aldama, M. Zajaček, B. Czerny, and S. Panda. Scatter Analysis along the Multidimensional Radius-Luminosity Relations for Reverberation-mapped Mg II Sources. *ApJ*, 903(2):86, November 2020, doi:10.3847/1538-4357/abb6f8.
- [15] D. Watson, K. D. Denney, M. Vestergaard, and T. M. Davis. A New Cosmological Distance Measure Using Active Galactic Nuclei. *ApJL*, 740:L49, October 2011, doi:10.1088/2041-8205/740/2/L49.
- [16] M. Haas, R. Chini, M. Ramolla, F. Pozo Nuñez, C. Westhues, and R. et al. Watermann. Photometric AGN reverberation mapping - an

- efficient tool for BLR sizes, black hole masses, and host-subtracted AGN luminosities. *A&A*, 535:A73, November 2011, doi:10.1051/0004-6361/201117325.
- [17] B. Czerny, J.-M. Wang, P. Du, K. Hryniewicz, V. Karas, Y.-R. Li, S. Panda, M. Śniegowska, C. Wildy, and Y.-F. Yuan. Interpretation of Departure from the Broad-line Region Scaling in Active Galactic Nuclei. *ApJ*, 870:84, January 2019, doi:10.3847/1538-4357/aaf396.
- [18] M. Zajaček, B. Czerny, M. L. Martínez-Aldama, M. Rałowski, A. Olejak, S. Panda, K. Hryniewicz, and et al. Time-delay Measurement of Mg II Broad-line Response for the Highly Accreting Quasar HE 0413-4031: Implications for the Mg II-based Radius-Luminosity Relation. *ApJ*, 896(2):146, June 2020, doi:10.3847/1538-4357/ab94ae.
- [19] R. Barlow. Asymmetric Statistical Errors. *arXiv e-prints*, page physics/0406120, June 2004.
- [20] P. Marziani and J. W. Sulentic. Highly accreting quasars: sample definition and possible cosmological implications. *MNRAS*, 442(2):1211–1229, August 2014, doi:10.1093/mnras/stu951.
- [21] J.-M. Wang, P. Du, C. Hu, H. Netzer, J.-M. Bai, K.-X. Lu, S. Kaspi, and SEAMBH Collaboration. Supermassive Black Holes with High Accretion Rates in Active Galactic Nuclei. II. The Most Luminous Standard Candles in the Universe. *ApJ*, 793:108, October 2014, doi:10.1088/0004-637X/793/2/108.
- [22] C. A. Negrete, D. Dultzin, P. Marziani, D. Esparza, J. W. Sulentic, A. del Olmo, M. L. Martínez-Aldama, and et al. Highly accreting quasars: The SDSS low-redshift catalog. *A&A*, 620:A118, Dec 2018, doi:10.1051/0004-6361/201833285.
- [23] J. W. Sulentic, A. del Olmo, P. Marziani, M. A. Martínez-Carballo, M. D’Onofrio, D. Dultzin, J. Perea, and et al. What does CIV λ 1549 tell us about the physical driver of the Eigenvector quasar sequence? *A&A*, 608:A122, December 2017, doi:10.1051/0004-6361/201630309.
- [24] M. L. Martínez-Aldama, A. del Olmo, P. Marziani, J. W. Sulentic, C. A. Negrete, D. Dultzin, and et al. Extreme quasars at high redshift. *A&A*, 618:A179, November 2018, doi:10.1051/0004-6361/201833541.
- [25] M. Śniegowska, P. Marziani, B. Czerny, S. Panda, M. L. Martínez-Aldama, and et al. High metal content of highly accreting quasars. *arXiv e-prints*, page arXiv:2009.14177, September 2020.
- [26] S. Panda, M. L. Martínez-Aldama, M. Marinello, B. Czerny, P. Marziani, and D. Dultzin. The CaFe Project: Optical Fe II and Near-infrared Ca II Triplet Emission in Active Galaxies. I. Photoionization Modeling. *ApJ*, 902(1):76, October 2020, doi:10.3847/1538-4357/abb5b8.
- [27] S. Panda. The CaFe Project: Optical Fe II and Near-Infrared Ca II triplet emission in active galaxies: (II) synthetic EWs, co-dependence between cloud sizes and metal content. *arXiv e-prints*, page arXiv:2004.13113, April 2020.
- [28] P. Du, K.-X. Lu, Z.-X. Zhang, Y.-K. Huang, K. Wang, C. Hu, J. Qiu, and SEAMBH Collaboration. Supermassive Black Holes with High Accretion Rates in Active Galactic Nuclei. V. A New Size-Luminosity Scaling Relation for the Broad-line Region. *ApJ*, 825:126, July 2016, doi:10.3847/0004-637X/825/2/126.
- [29] S. Panda, P. Marziani, and B. Czerny. The Quasar Main Sequence Explained by the Combination of Eddington Ratio, Metallicity, and Orientation. *ApJ*, 882(2):79, Sep 2019, doi:10.3847/1538-4357/ab3292.
- [30] D. Dultzin, P. Marziani, J. A. de Diego, C. A. Negrete, A. Del Olmo, M. L. Martínez-Aldama, and et al. Extreme quasars as distance indicators in cosmology. *Frontiers in Astronomy and Space Sciences*, 6:80, January 2020, doi:10.3389/fspas.2019.00080.
- [31] Y. Shen, P. B. Hall, K. Horne, G. Zhu, I. McGreer, T. Simm, and et al. The Sloan Digital Sky Survey Reverberation Mapping Project: Sample Characterization. *ApJS*, 241(2):34, April 2019, doi:10.3847/1538-4365/ab074f.
- [32] M.-H. Naddaf, B. Czerny, and R. Szczerba. BLR size in Realistic FRADO Model. *Frontiers in Astronomy and Space Sciences*, 7:15, April 2020, doi:10.3389/fspas.2020.00015.

- [33] A. G. Riess, S. Casertano, W. Yuan, L. Macri, B. Bucciarelli, M. G. Lattanzi, J. W. MacKenty, and et al. Milky Way Cepheid Standards for Measuring Cosmic Distances and Application to Gaia DR2: Implications for the Hubble Constant. *ApJ*, 861:126, July 2018, doi:10.3847/1538-4357/aac82e.
- [34] E. Lusso, G. Risaliti, E. Nardini, G. Bargiacchi, M. Benetti, S. Bisogni, S. Capozziello, and et al. Quasars as standard candles. III. Validation of a new sample for cosmological studies. *A&A*, 642:A150, October 2020, doi:10.1051/0004-6361/202038899.